Magnetic relaxation in $YBa_2Cu_3O_x$

Donglu Shi and S. Salem-Sugui, Jr.
Materials Science Division, Argonne National Laboratory, Argonne, Illinois 60439
(Received 13 May 1991; revised manuscript received 27 June 1991)

We measured the magnetic relaxation in the high-T_c superconductor $YBa_2Cu_3O_x$ at a wide range of temperatures and applied fields. The relaxation measurements were performed on single-crystal, melt-textured, and sintered samples. We found that magnetic relaxation depends strongly on the microstructure and crystal orientation. By combining Bean's critical-state model and the Anderson-Kim flux-creep theory, we used a previously developed expression to interpret the magnetic relaxation behavior and the dependence of the field penetration on the sample size. We also investigated the relationship between the flux-creep-activation pinning energy and the decay of the persistent current in the single-crystal sample of $YBa_2Cu_3O_x$.

I. INTRODUCTION

Magnetic relaxation has been observed in type-II superconductors including high-T_c oxides.[1-9] The origin of the time dependence of the current decay was long ago interpreted by a thermally activated flux-creep theory proposed by Anderson and Kim (Anderson-Kim model).[10] It is assumed in this model that an Abrikosov flux line or flux bundle can be thermally activated and jump over the pinning barriers. The hopping rate can be described by an Arrhenius law. According to this theory, the magnetization in a type-II superconductor will decay logarithmically as a function of time. Beasley, Labusch, and Webb[8] experimentally investigated the Anderson-Kim model to describe the flux-creep behavior in conventional systems. In their study, the concept of critical state was used to discuss the flux dynamics in type-II superconductors. The slow decay of the persistent current from the critical state was shown to be an indication of thermally activated flux creep. More specifically, Beasley, Labusch, and Webb observed $\ln(t)$ decay of magnetization and studied the flux-creep rates associated with thermal activation processes in the mixed state. They also discussed the relationship between the effective pinning energy, U, and persistent current and obtained an expression of U with certain approximations. However, it has not been clear whether these approximations are appropriate in high-T_c systems, although the expressions have been extensively used for high-T_c superconductors. More important, nonlogarithmic time decay of magnetization has been reported in many high-T_c superconductors,[6,7,11] which cannot be easily described by the Anderson-Kim model.

From the classical Anderson-Kim theory and considering the possibility of reverse flux hopping, the hopping rate, ν, can be written as

$$\nu=\nu_0 \sinh(JU_0/J_0kT)\exp(-U_0/kT)\ , \tag{1}$$

where ν_0 is the attempt frequency, J is the apparent critical-current density, J_0 is the Bean critical current density in the absence of flux creep, and U_0 is the apparent pinning energy. Three models have been proposed to interpret the nonlogarithmic time decay of magnetization. In the thermally activated flux flow (TAFF), Kes *et al.*[12] assumed that for $J \ll J_0$ the sinh term could be approximated by (JU_0/J_0kT). Therefore, the persistent current, J, should decay exponentially in the limit of $J \ll J_0$. The TAFF model interprets the observed nonlogarithmic decay as a crossover from Anderson-Kim $\ln(t)$ decay to exponential decay, where the crossover time t_{cr} is of $(1/\nu_0)\exp(-U/kT)$. In a model based on the concept of collective creep, Feigel'man *et al.*[13] proposed a decay $J(t)=J_0[U_0/kT\ln(t/t_0)]^{1/\alpha}$, $t_0 \sim 1/\nu_0$. Although the TAFF and collective creep models have different forms of current decay, they are both based on the same physical foundation of thermally activated flux creep, and both assume that the measured $J \ll J_0$. A third model, developed by Fisher,[14] predicts a similar current decay in a three-dimensional vortex glass phase.

Most recently, Ling, Shi, and Budnick[15] proposed a fundamentally different interpretation for the decay of the persistent current in type-II superconductors. They showed that the nonlogarithmic time dependence of magnetization is associated with the so-called self-organized criticality.[16,17] They successfully demonstrated that the magnetic relaxation in both conventional and high-T_c superconductors can be described by a stretched exponential function, which has been observed in the sandpile process.[17,18]

In this paper, we show magnetic relaxation data obtained over wide temperature and field regions for the high-T_c superconductor $YBa_2Cu_3O_x$. The samples chosen for this study are flux-grown single-crystal, melt-textured, and sintered polycrystalline ceramics. We show that the magnetic relaxation is strongly affected by many factors of the materials such as orientation, size, grain boundary weak links, and pinning characteristics. In turn, the superconducting properties such as critical current density, temperature and current dependences of pinning energy, and field penetration are also closely connected with these factors. Using a model we previously developed based on thermally activated flux creep,[5] we

interpret the magnetic relaxation behavior in these samples. We also discuss the relationship between the effective pinning energy and persistent current in the $YBa_2Cu_3O_x$ single crystal.

II. EXPERIMENTAL PROCEDURE

The single crystal (SC) of $YBa_2Cu_3O_x$ measuring $1\times2\times0.1$ mm^3 was grown by a flux method. The melt-textured (MT) and sintered (ST) samples were made by a partial-melting process and conventional ceramic method, respectively.[19–21] X-ray diffraction showed that samples were of single phase. The zero-field-cooled magnetization at 20 G exhibited a sharp transition near 90 K for the SC and MT samples.

Magnetization measurements were carried out on a Quantum Design SQUID magnetometer. The samples were first zero-field-cooled to a desired temperature, T, below the transition temperature, T_c. A magnetic field, H, was then applied normal to the a-b plane of the single-crystal and melt-textured samples. The magnetization, M, of the samples was measured as a function of time, t. The initial data point of the magnetization was taken at $t_0=180$ s. Using standard procedures with the commercial SQUID, we cannot get relaxation information earlier than 100 seconds after the field is settled. The travel length of the sample in each scan was 3 cm for all measurements to avoid field inhomogeneity.

III. RESULTS

We first show magnetic relaxation data for the SC [Fig. 1(a)], MT [Fig. 1(b)], and ST [Fig. 1(c)] samples at 20 kG and temperatures indicated. The common feature of these curves is that the magnetization decreases linearly as a function of $\ln(t)$. As can be seen in Fig. 1, the slope of the magnetic relaxation, S $(=dM/d\ln t)$, varies considerably at different temperatures.

In Fig. 2 we plot S versus applied field, H, for the SC [Fig. 2(a)], ST [Fig. 2(b)] samples at temperature $T=20$, 30, and 40 K. It can be seen in this figure that S begins with a very small value and then increases with increasing field. As shown in Fig. 2(a) for SC, S at all temperatures gradually increases to a certain value and then saturates at almost a constant. However, the field at which S saturates (denoted here as H^*) varies with temperature. Quite different behavior is observed for the ST sample. As shown in Fig. 2(b), the initial increase of S is much more rapid, and the S versus H curves all exhibit "peaks" (H^*) at various field values. Further, the peaks of the ST samples occur at much lower field values than those of SC. For example, H^* at 20 K is around 8 kG for SC but near 3 kG for ST. We note that H^* has been previously identified[5] as the field at which the sample is first fully penetrated.

To study the effect of sample size on the magnetic relaxation and the field penetration, we powdered the melt-textured sample to fine particles with an average diameter $d=5-10\mu$m. In Fig. 3(a) we plot S versus applied field for the single-crystal (SC) and sintered (ST) samples; in Fig. 3(b), we plot results for the bulk melt-textured (MT) and powdered sample (MTPW). We see that MTPW has much smaller H^* values than those of MT. We also see from Fig. 3 that the samples are easily penetrated by the magnetic field when the sample has

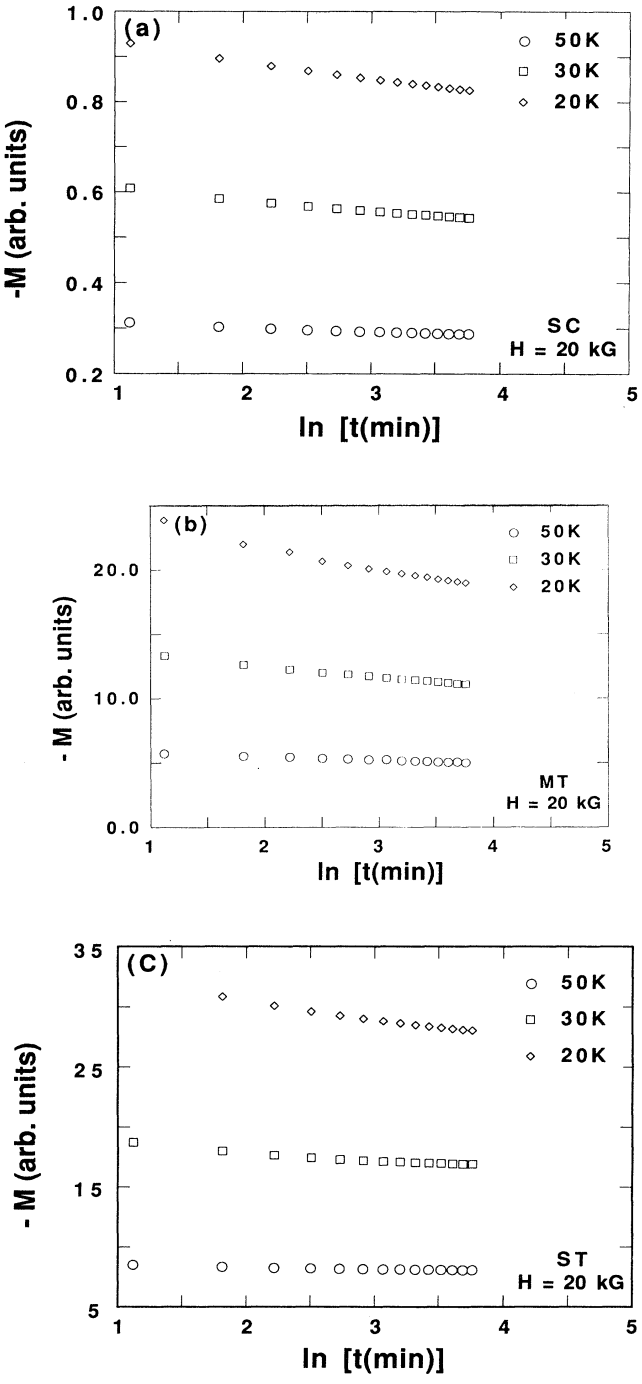

FIG. 1. Magnetization vs $\ln(t)$ at a given field $H=20$ kG for (a) single-crystal (SC), (b) melt-textured (MT), and (c) sintered (ST) $YBa_2Cu_3O_x$ at temperatures indicated. The field, parallel to the c axis for SC and MT, is applied after cooling the sample in zero field.

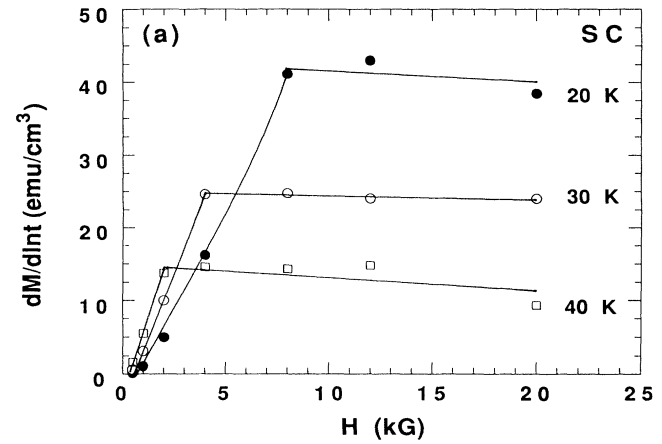

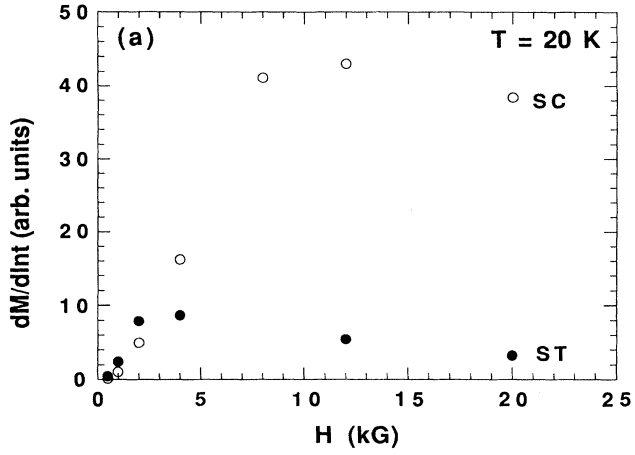

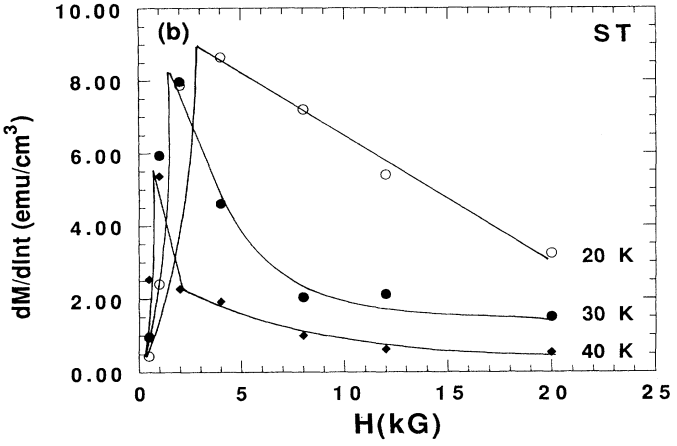

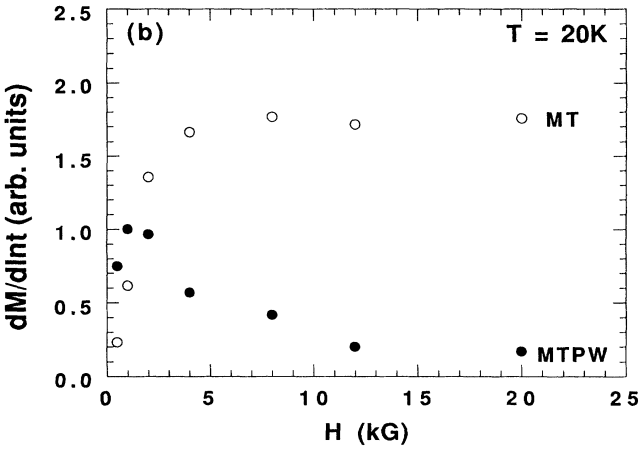

FIG. 2. S ($=dM/d\ln t$) vs. applied field for (a) single-crystal and (b) sintered (ST) $YBa_2Cu_3O_x$ at temperatures indicated. The solid lines are a guide for the eye.

FIG. 3. S ($-dM/D\ln t$) vs. applied field at 20 K for (a) single-crystal (SC) and sintered (ST) and (b) bulk melt-textured (MT) and powdered melt-textured (MTPW) $YBa_2Cu_3O_x$.

grain boundaries (ST) or very small sizes (MTPW). The H^* versus T data for all the samples (SC, ST, MT, and MTPW) are shown in Fig. 4.

IV. DISCUSSION

A. Magnetic relaxation behavior

Magnetic relaxation in SC has been previously interpreted by Yeshurun *et al.*[2,3] based on Anderson's classic flux-creep model.[10] High, thermally activated flux creep results in magnetic relaxation and decay of the current density. As was previously reported,[5] the Bean model[22] can be combined with an expression for the time decay of persistent current developed by Campbell and Evetts:[23]

$$J_c(T)=J_0[1-(kT/U_0)\ln(t/t_0)]\ , \tag{2}$$

where J_0 is the critical current density when no thermal disturbance is present, $1/t_0$ is the attempt frequency for the flux lines to jump over the pinning well, and U is the effective pinning energy for the motion of the flux lines. For simplicity, the following formula is used to express the field dependence of J_c under the condition $H_i \ll H_0$:[5]

$$J_c(T,H_i)=J_c(T)(1-H_i/H_0)\ , \tag{3}$$

where H_i is the local field, and H_0 is a materials parameter with a magnetic field dimension that can be determined experimentally. This formula is particularly relevant for superconductors with relatively high H_0 values.[5]

In a critical state we have

$$-dH_i/dx=4\pi J_c(H_i)/c\ , \tag{4}$$

where c is the speed of light (we use the Gaussian unit throughout the paper). Considering a slab of thickness D with the field perpendicular to the direction of the current and assuming H_{c1} to be negligible, the following expression can be derived for the local field, H_i,

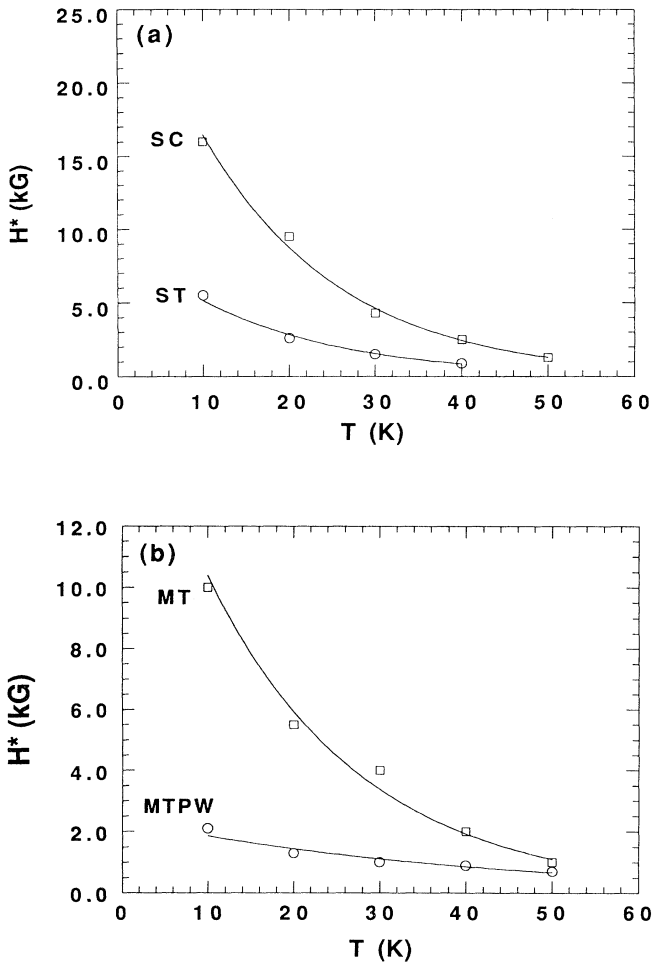

FIG. 4. Penetration field H^* vs. T for (a) single-crystal (SC) and sintered (ST) and (b) bulk melt-textured (MT) and powdered melt-textured (MTPW) $YBa_2Cu_3O_x$. The solid lines are a guide for the eye.

$$H_i(x)=H_0-(H_0-H)\exp(x/x_0)\ , \tag{5}$$

where $x_0=cH_0/4\pi J_c(T)$ and H is the applied magnetic field. The average magnetic induction is given by

$$\langle B\rangle=-H_0\frac{2x_0}{D}\ln\left[1-\frac{H}{H_0}\right]-\frac{2x_0}{D}H,\quad H<H^*\ , \tag{6a}$$

$$\langle B\rangle=H_0+\frac{2x_0}{D}\left[\exp\left[\frac{D}{2x_0}\right]-1\right](H-H_0),\quad H>H^*\ , \tag{6b}$$

where $H^*=H_0[1-\exp(-D/2x_0)]$. Substituting Eq. (2) into Eq. (6) and knowing that the magnetization $4\pi M$ is given by $\langle B\rangle-H$, the derivative of the magnetization with respect to time to the first-order approximation in kT/U_0 can be obtained:

$$4\pi dM/d\ln t=a(H^2/H_0)(kT/U_0),\quad H<H^*\ , \tag{7a}$$

$$4\pi dM/d\ln t=b(-H+H_0)(kT/U_0),\quad H>H^*\ , \tag{7b}$$

where $a=x_0/D$, and $b=(2x_0/D)\{1+[(D/2x_0)-1]\exp(D/2x_0)\}$. From Eq. (7a) we can see that $dM/d\ln t$ should increase as H^2 in the field region $H<H^*$. When the sample has been fully penetrated by the applied field ($H>H^*$) as described by Eq. (7b), $dM/d\ln t$ exhibits a linear decrease with increasing field. This behavior has been found in the Bi-Sr-Ca-Cu-O system.[5] Although, in this study, we do not have enough data points in the region of $H<H^*$ to fit Eq. (7), the general trend of $dM/d\ln t$ shown in Fig. 2 is quite agreeable with that model.

As shown in Fig. 2(a) for SC, $dM/d\ln t$ has a clear linear dependence on H in the $H>H^*$ region. However, as shown in Fig. 2(b), this linear dependence may be suppressed in the regions near H^* for the ST sample (there are not enough data points to verify this) at high temperatures ($T=30$ and 40 K). This behavior can be interpreted by the condition $H_i\ll H_0$ in the modified Bean critical-state model [Eq. (3)]. As we pointed out before, H_0 is a materials parameter with a magnetic field dimension, which may correspond to the critical fields of the superconductor (H_{c1}, H_c, and H_{c2}). At high temperatures and fields, H_0 is considerably reduced, therefore, the condition $H_i\ll H_0$ is no longer satisfied. Indeed, Kim, Hempstead, and Strnad[24] have reported that H_0 is approximately equal to the thermodynamic critical field H_c ($\sim 1-t, t=T/T_c$) for Nb_3Sn and Nb-Zr superconductors. Thus, experimental data could severely deviate from Eq. (3) as the condition $H_i\ll H_0$ is not satisfied. As can be seen in Fig. 2(b), the linearity of field dependence of $dM/d\ln t$ no longer exists at high temperatures and fields. It should be noted that different field dependences of J_c have been reported for various superconducting systems such as the Kim model[24] $[J_c(T,H_i)=J_c(T)/(1+H_i/H_0)]$, the power-law $[J_c(T,H_i)=J_c(T)(H_i/H_0^{-n})]$,[25] and the exponential $[J_c(T,H_i)=\exp(-H_i/H_0)]$ (Ref. 26) relations. Using these relations, we have previously developed expressions of $dM/d\ln t$ without the approximation $H_i\ll H_0$, which give nonlinear field dependence in the $H>H^*$ region.[27]

B. Effect of sample size on H^*

As indicated above, $H^*=H_0[1-\exp(-D/2x_0)]$, where $x_0=cH_0/4\pi J_c(T)$. It is obvious that the condition $D/2x_0\ll 1$ is equivalent to $H_0\gg 2\pi J_c(T)D/c$. The term $\exp(-D/2x_0)$ can be expanded to be $(1-D/2x_0)$ as we take the first-order approximation for $D/2x_0\ll 1$ at relatively low temperature and field regions.[5] Therefore, $H^*=H_0D/2x_0$ (i.e., H^* should be proportional to sample size D). It has been shown in Figs. 2 and 3 that the H^* values of MTPW and ST are much smaller than those of MT and SC. These results are consistent with our hypothesis. For the melt-textured samples, the sample size D is largely reduced in the MTPW sample ($D\sim 5$–10 μm) compared to that of the MT sample

($D \sim 2$ mm), thus resulting in smaller H^* in the MTPW. For the ST sample, although the bulk size ($D \sim 1.5$ mm) is comparable to that of the SC, the grain boundaries are easily penetrated by the applied magnetic field at the decoupling field of Josephson junctions (a few hundred Gauss for $YBa_2Cu_3O_x$.[28] Thus, the effective size for the sintered sample is the grain size, which is on the order of 20 μm. Consistently, H^* of ST is also much lower than that of the SC, since no grain boundaries exist in the single crystal. Thus, we have shown that the H^* is indeed the full penetration field and depends upon the dimension of the samples. For weakly linked materials, H^* is directly related to the size of the regions (grains) which are coupled by the Josephson junction.

It should be pointed out that there has been a misconception about melt-textured $YBa_2Cu_3O_x$ having a high levitation force as a result of strong pinning effects. Based on our discussion, we conclude that the relatively larger levitation force observed from the melt-textured $YBa_2Cu_3O_x$ is partially attributable to the fact that it is difficult for the field to penetrate the textured samples with high H^* values (i.e., the grain boundaries in the melt-textured $YBa_2Cu_3O_x$ are strongly coupled). It has been well reported that the intragranular pinning also contributes to high critical current density and levitation force.[29]

C. Activation pinning energy for flux creep

Activation energy for flux creep has been extensively studied for the high-T_c systems.[2,4,7,8,30] However, because of the complex relationships between various superconducting parameters, it has not been clear how the activation pinning energy can be determined from the flux-creep data. We thus attempted to investigate this problem based on our experimental data and previously reported results.

Beasley, Labusch, and Webb[8] derived an expression for flux creep R ($=d\phi/d\ln t$, where ϕ is the total flux in the sample) based on the Anderson thermally activated flux-creep theory in which the flux hopping frequency ν is given by

$$\nu = \nu_0 \exp(-U/kT) , \tag{8}$$

where ν_0 is an attempt frequency and U is an effective activation energy. According to the conservation of flux,

$$\partial \mathbf{B}/\partial t = -\nabla \mathbf{D} , \tag{9}$$

where $\mathbf{D}$ is the flux-flow density. Thus, the one-dimensional flux-creep equation can be written as

$$\frac{\partial B}{\partial t} \nabla [(\nabla B/|\nabla B|) B a \nu_0 \exp(-U/kT)] , \tag{10}$$

where a is the flux hopping distance and B is the magnetic induction. Equation (10) can be solved by assuming $U \gg kT$. The flux creep R is given by

$$R = \pm \tfrac{1}{3} \pi k T \rho^3 [(\partial U/|\nabla B|)_{t,\rho}]^{-1} (1 \pm \delta) , \tag{11}$$

where ρ is the sample radius and δ is a correction factor, which is small compared to unity. Beasley, Labusch, and Webb[8] pointed out that U should be a nonlinear function of ∇B, as a result of thermal activation at the top of the energy barrier (see Fig. 5). A possible solution for Eq. (11) can be obtained graphically by the tangent of the U versus ∇B curve as represented in Fig. 5. This solution has the form

$$\left[\frac{\partial U}{\partial (\nabla B)} \right]_{t,\rho} = \frac{U_0 - U(J)}{\frac{4\pi J}{c}} , \tag{12}$$

where J is the current density and U_0 is called apparent activation energy since it is obtained by a linear approximation. The linear graphic solution above corresponds to the Anderson-Kim expression for the effective pinning energy,

$$U = U_0 - |F| V X , \tag{13}$$

where F is the driving force, V is the activation volume and X is the pinning length. With an additional approximation made by Beasley, Labusch, and Webb that $U_0 \gg U$, the final solution for the apparent pinning energy can be expressed as

$$\frac{1}{M_0} (dM/d\ln t) = -\frac{kT}{U_0} , \tag{14}$$

where M_0 is the magnetization in the absence of flux

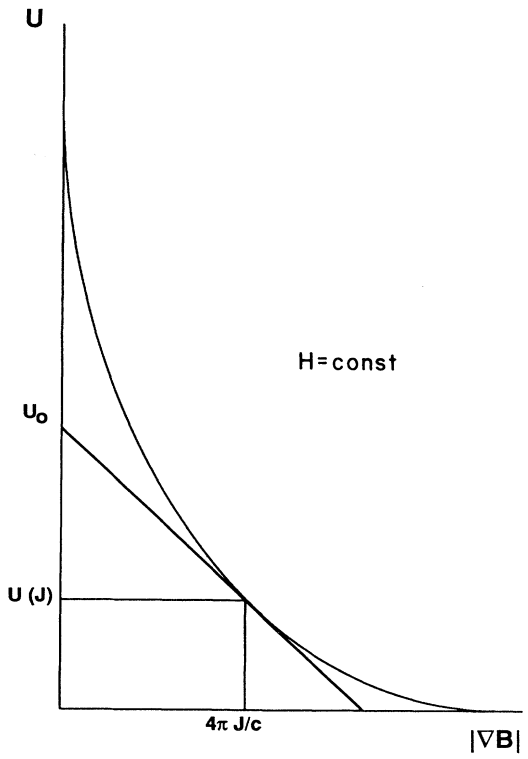

FIG. 5. Schematic plot showing the nonlinear current dependence of the effective pinning energy, U. The tangent line indicates the linear approximation and graphic solution used in Ref. 8 for obtaining the apparent pinning energy, U_0.

creep. Equation (14) has been used extensively to calculate U_0 based on magnetic relaxation measurements. However, there are serious problems in using Eq. (14), which will be addressed in detail later.

The nonlinear behavior, illustrated in Fig. 5, has been experimentally observed from resistivity measurements in $YBa_2Cu_3O_x$ thin films by Zeldov *et al.*,[31] and from magnetic relaxation measurements in grain-aligned $YBa_2Cu_3O_x$ by Maley *et al.*[32] In both studies, the researchers have observed a logarithmic dependence of U on J.

With a different approach from Ref. 32, Maley *et al.* developed an expression for the effective pinning energy U, which can be written as

$$U/k = -T \ln |dM/dt| + T \ln(Bva/\pi d) , \quad (15)$$

where a is the flux hopping distance and d is the thickness of the sample. It should be noted that Eq. (15) was obtained without the approximation $U \gg kT$.

In the following we use the same approach as developed by Maley *et al.* to obtain U as a function of $J \sim -M$, for the $YBa_2Cu_3O_x$ single crystal. We first calculated $T \ln|dM/dt|$ for various temperatures at a given field. Then, by adjusting the constant $C = \ln(Bva/\pi d)$, we obtained a smooth $U/(1-T/T_c)^{3/2}$ versus M curve. The curves at 8, 12, and 20 kG are presented in Fig. 6. To obtain the best value of C, we used a scaling factor of U, $(1-T/T_c)^{3/2}$, as discussed by McHenry *et al.*[33] We found that the value of $C = 12$ gives the best fit for all the curves presented in Fig. 6.

Our value of C ($=12$) seems to be consistent with the value ($C = 18$) obtained by Maley *et al.* for the grain-aligned $YBa_2Cu_3O_x$. We found that the difference in C values is associated with the fact that d ($=12$ μm) is the grain size in their study but is the sample size ($d \sim 1$ mm) in our experiments. The curve fitting also give a power-law dependence of U: $U \sim |M|^{-\mu}$, where $\mu \sim 1.2$–1.5 for all the applied fields indicated (Fig. 6). This power-law relation was predicted by Feigel'man *et al.* in the collective creep model.[13] However, this is in contrast to the observations ($U \sim \ln |M|$) of Zeldov *et al.*[31] and Maley *et al.* in the same superconducting system: $YBa_2Cu_3O_x$.[32]

The apparent pinning energy U_0 of the $YBa_2Cu_3O_x$ single crystal is plotted against T at 12 kG as shown in Fig. 7. Consistent with the previously reported data,[7,11] U_0 increases with increasing temperature. In Table I, we present values of U and U_0 at $1.2T$ and various temperatures indicated for SC. The average values of U are calculated by using Eq. (15) with the fitting constant $C = \ln(Bva/\pi d) = 12$. As shown in Table I, U increases as a function of temperature between 10 and 50 K. According to Beasley *et al.*,[8] U approaches U_p, the intrinsic pinning energy, as J is reduced to zero. However, physically, U should go to zero at T_c. Since our data were taken in the temperature range well below T_c, we only observed U increasing with T. The U_0 values are calculated by using Eq. (14). We mentioned before that Eq. (14) was developed with an assumption that $U_0 \gg U$. However, a comparison of the U and U_0 values presented in Table I shows that they are rather close to each other. This result implies that the condition $U_0 \gg U$ is not satisfied for SC. Thus, U_0 has no well-defined physical meaning for the high-T_c oxides. It is particularly not appropriate to compare U_0 values calculated by using Eq. (14) among different superconducting systems.

V. CONCLUSIONS

We measured the magnetic relaxation in various forms of $YBa_2Cu_3O_x$ (single-crystal, melt-textured, and sintered samples) at various temperatures and applied fields. We found that magnetic relaxation is strongly affected by the microstructure, crystal orientation, and pinning characteristics of the samples. We used a previously developed expression to interpret the flux-creep behavior and mag-

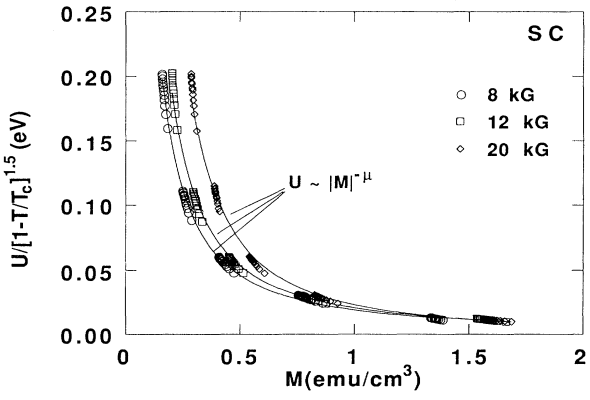

FIG. 6. Effective pinning energy U is plotted against magnetization for the single crystal of $YBa_2Cu_3O_x$ for H parallel to the c axis at the field values indicated. The solid lines are the fit of the U data at $T = 10$, 20, 30, 40, and 50 K to Eq. (15). The best fit is obtained by adjusting the constant C [$= T \ln(Bva/\pi d) = 12$].

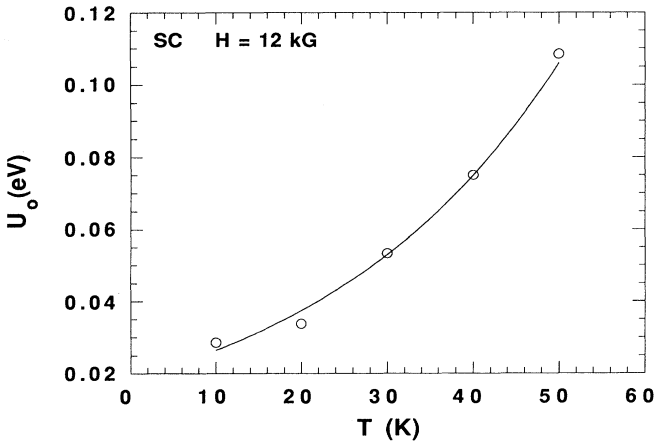

FIG. 7. Apparent pinning energy U_0 vs T at 12 kG for the $YBa_2Cu_3O_x$ single crystal. Note that the U_0 values are calculated by using Eq. (14).

TABLE I. Values of effective pinning energy U and apparent pinning energy U_0 at 12 kG and various temperatures for the single cyrstal of $YBa_2Cu_3O_x$. U_0 and U are calculated using Eqs. (14) and (15), respectively. The field is parallel to the c axis.

T (K)	10	20	30	40	50
U (eV)	0.015	0.028	0.045	0.064	0.079
U_0 (eV)	0.029	0.034	0.053	0.075	0.108

netic field penetration. We found that the full penetration field H^* is sensitively dependent on the sample size and on weakly coupled Josephson junctions. It is quite easy for the field to penetrate samples with small dimensions and weak-link boundaries. It is difficult to obtain the activation pinning energy based on the flux-creep measurements, and the apparent pinning energy U_0 introduced by Beasley *et al.* is not well defined physically in high-T_c systems.

ACKNOWLEDGMENTS

We are grateful to Ming Xu for useful discussions during this research. This work was supported by the U.S. Department of Energy, Basic Energy Sciences–Materials Sciences, under Contract No. W-31-109-ENG-38. S.S.S. acknowledges financial support from Fundação de Amparo a Pesquisa do Estado de São Paulo, FAPESP, Brazil.

[1]K. A. Muller, M. Takashige, and J. G. Bednorz, Phys. Rev. Lett. **58**, 1143 (1987).
[2]Y. Yeshurun and A. P. Malozemoff, Phys. Rev. Lett. **60**, 2202 (1988).
[3]Y. Yeshurun, A. P. Malozemoff, T. K. Worthington, R. M. Yandrofski, L. Krusin-Elbaum, F. H. Holtzberg, T. R. Dinger, and G. V. Chandrashekhar, Cryogenics **29**, 258 (1989).
[4]Donglu Shi, X. S. Ling, Ming Xu, M. M. Fang, Sheng Luo, J. I. Budnick, B. Dabrowski, D. G. Hinks, D. R. Richards, and Y. Zheng, Phys. Rev. B **43**, 3684 (1991).
[5]D. Shi, M. Xu, A. Umezawa, and R. F. Fox, Phys. Rev. B **42**, 2062 (1990); Ming Xu, Donglu Shi, A. Umezawa, K. G. Vandervoort, and G. W. Crabtree, *ibid.* **43**, 13 049 (1991).
[6]Donglu Shi and Ming Xu, Phys. Rev. B **44**, 4548 (1991).
[7]Youwen Xu, M. Suenaga, A. R. Moodenbaugh, and D. O. Welch, Phys. Rev. B **40**, 10 882 (1989).
[8]M. R. Beasley, R. Labusch, and W. W. Webb, Phys. Rev. **181**, 682 (1969).
[9]M. Suenaga, A. K. Ghosh, Youwen Xu, and D. O. Welch, Phys. Rev. Lett. **66**, 1777 (1991).
[10]P. W. Anderson, Phys. Rev. Lett. **9**, 309 (1962).
[11]Y. Xu, M. Suenaga, Y. Gao, J. E. Crow, and N. D. Spencer, Phys. Rev. B **42**, 8756 (1990).
[12]P. H. Kes, J. Aarto, J. van den Berg, C. J. van der Beek, and J. A. Mydosh, Supercond. Sci. Technol. **1**, 242 (1989).
[13]M. V. Feigel'man, V. B. Geshkenbein, A. I. Larkin, and V. M. Vinokur, Phys. Rev. Lett. **63**, 2303 (1989); A. I. Larkin and Yu N. Ovchinnikov, J. Low Temp. Phys. **34**, 409 (1979).
[14]M. P. A. Fisher, Phys. Rev. Lett. **62**, 1415 (1989).
[15]S. X. Ling, Donglu Shi, and J. I. Budnick (unpublished).
[16]P. Bak, C. Tang, and K. Wiesenfeld, Phys. Rev. Lett. **59**, 381 (1987).
[17]C. Tang and P. Bak, Phys. Rev. Lett. **60**, 2347 (1988).
[18]J. M. Carlson *et al.*, Phys. Rev. Lett. **65**, 2547 (1990).
[19]D. Shi, H. Krishnan, J. M. Hong, D. Miller, P. J. McGinn, W. H. Chen, M. Xu, J. G. Chen, M. M. Fang, U. Welp, M. T. Lanagan, K. C. Goretta, J. T. Dusek, J. J. Picciolo, and U. Balachandran, J. Appl. Phys. **68**, 228 (1990).
[20]D. Shi, M. M. Fang, J. Akujieze, M. Xu, J. G. Chen, and C. Segre, Appl. Phys. Lett. **57**, 2606 (1990).
[21]D. Shi, D. W. Capone II, G. T. Goudey, J. P. Singh, N. J. Zaluzec, and K. C. Goretta, Mater. Lett. **6**, (7), 217 (1988).
[22]C. P. Bean, Phys. Rev. Lett. **8**, 250 (1962); Rev. Mod. Phys. **36**, 31 (1964).
[23]A. M. Cambell and J. E. Evetts, Adv. Phys. **21**, 199 (1972).
[24]Y. B. Kim, C. F. Hempstead, and A. R. Strnad, Phys. Rev. Lett. **9**, 306 (1962); Phys. Rev. **129**, 528 (1963).
[25]H. A. Ullmaier and R. H. Kernohan, Phys. Status Solidi **17**, K223 (1966).
[26]W. A. Feitz, M. R. Beasley, J. Sicox, and W. W. Webb, Phys. Rev. A **335**, 136 (1964).
[27]M. Xu and D. Shi, Physica C **168**, 303 (1990).
[28]R. B. Stephens, Cryogenics **29**, 399 (1989).
[29]M. Murakami, T. Oyama, H. Fujimoto, T. Taguchi, S. Gotoh, Y. Shiohara, N. Koshizuka, and S. Tanaka, Jpn. J. Appl. Phys. **29**, L1991 (1990).
[30]T. T. M. Palstra, B. Batlogg, R. B. van Dover, L. F. Schneemeyer, and J. V. Waszczak, Phys. Rev. B **41**, 6621 (1990); T. T. M. Palstra, B. Batlogg, L. F. Schneemeyer, and J. V. Waszczak, Phys. Rev. Lett. **61**, 1662 (1988).
[31]E. Zeldov, N. N. Amer, G. Koren, A. Gipta, M. W. McElfresh, and R. J. Gambino, Appl. Phys. Lett. **56**, 680 (1990).
[32]M. P. Maley, J. O. Willis, H. Lessure, and M. E. McHenry, Phys. Rev. B **42**, R2639 (1990).
[33]M. E. McHenry, S. Simizu, H. Lessure, M. P. Maley, Y. C. Coulter, I. Tanaka, and H. Kojima (unpublished).